Friction-controlled bending solitons as folding pathway toward colloidal clusters

2010 EPL 90 58001

(http://iopscience.iop.org/0295-5075/90/5/58001)

A Letters Journal Exploring the Frontiers of Physics

June 2010

EPL, **90** (2010) 58001
doi: 10.1209/0295-5075/90/58001

www.epljournal.org

Friction-controlled bending solitons as folding pathway toward colloidal clusters

N. Casic[1], S. Schreiber[1], P. Tierno[2], W. Zimmermann[1] and T. M. Fischer[1(a)]

[1] *Institute of Physics, Universität Bayreuth - 95440 Bayreuth, Germany, EU*
[2] *Departament de Química Física, Universitat de Barcelona - Martí i Franquès 1, 08028 Barcelona, Spain, EU*

received 4 May 2010; accepted in final form 1 June 2010
published online 17 June 2010

PACS 82.70.Dd – Colloids
PACS 87.15.hm – Folding dynamics
PACS 87.15.hp – Conformational changes

Abstract – We study the conformational transition of an ensemble of magnetic particles from a linear chain to a compact cluster when subjected to an external magnetic field modulation. We show that the transient dynamics induced by switching the field from static to rotating is governed by the relative friction of adjacent particles in the chain. Solid particles show bending solitons counter-propagating along the chain while buckling of the chain is the mechanism preferred by ferrofluid droplets. By combining real-space experiments with numerical simulations we unveil the underlying mechanism of folding pathways in driven colloidal systems.

Folding pathways in conformational space are crucial to understand protein folding [1]. The pathway of a protein from its unfolded to the biological relevant folded conformation has been described as a statistical path through the multi-dimensional energy landscape in conformational space. Rate-determining regions of such paths are the saddle points in the energy landscape passed by the folding pathway [2]. More than one saddle point generically leads to a multi-exponential relaxation process. Cross correlations of stochastic forces occurring due to the collision of solvent molecules with the protein give rise to hydrodynamic friction forces which could affect the chosen pathway. Hydrodynamic friction may thus play an important role in polymer [3] and protein [4] folding by speeding up the folding process.

Colloidal suspensions are mesoscopic systems, where complex structures and dynamics resulting from simple and tuneable interactions between individual particles can be studied in real space. Thus they have been used as models for crystalline assemblies [5], glasses [6], van der Waals crystals [7], phononic crystals [8] and dipolar chains [9]. Colloidal chains might, however, also serve as a model system for folding pathways. We show that for paramagnetic colloidal chains interacting via time-averaged dipolar interactions not only the speed of folding [3,4], but also the selection of the folding pathway is controlled by the complexity of the friction between the particles during the conformational transition.

Here we report on the conformational change of a 2D assembly of magnetic particles from a pearl chain to a cluster. We realize a 1D chain by applying a static magnetic field and force the particles into a 2D compact cluster by suddenly switching from a static to a rotating field. At high rotation frequencies, the pearl chain curls up into two spirals wrapping the chain into a cluster. We show that the dynamics of the curling-up of the pearl chain can be understood by two localized bending solitons moving from both ends of the pearl chain toward the center. The longer folding pathway via the bending solitons is preferred over the shortest pathway consisting of a buckling of the chain, the latter being suppressed by the friction between adjacent particles.

Our experiment employs two types of water-dispersed magnetic particles confined by gravity on a solid substrate: paramagnetic colloidal particles (Dynabeads M-270, radius $a = 1.4\,\mu$m) and SDS stabilized ferrofluid droplets (APG-820 Ferrofluid). The paramagnetic colloids were diluted in Millipore water ($5 \cdot 10^{-6}$ beads/ml) while the ferrofluid emulsion was prepared by dispersing 6% by w. of APG into a water solution containing 1.6% by w. of SDS. We apply an external magnetic field using two coils perpendicular to each other ($\mathbf{e}_x$, $\mathbf{e}_y$ directions), mounted on an optical microscope (see [10] for more experimental details).

(a) E-mail: thomas.fischer@uni-bayreuth.de

In a rotating magnetic field of angular frequency ω, $\mathbf{H} = H(\cos\omega t\mathbf{e}_x + \sin\omega t\mathbf{e}_y)$, the particles acquire a magnetic moment $\mathbf{m}(\omega) = V\chi(\omega)\cdot\mathbf{H}(\omega)$ proportional to the field, with V being the particle volume and $\chi(\omega)$ the effective dynamic magnetic susceptibility. The dipolar interaction energy between the induced moments of two equal particles located at $\mathbf{r}_1(t)$ and $\mathbf{r}_2(t)$ is

$$W = -\frac{\mu_0}{4\pi}\mathbf{m}(\mathbf{r}_1(t))\mathbf{m}(\mathbf{r}_2(t)):\frac{3\mathbf{r}(t)\mathbf{r}(t) - r^2\mathbf{1}}{r^5}, \qquad (1)$$

where $\mathbf{r}(t) = \mathbf{r}_1(t) - \mathbf{r}_2(t)$ is the separation of the dipoles. Such interaction results in a relative particle motion at a typical shear rate of magnitude Ω. The dimensionless Mason number $\mathcal{M} = \eta\omega/\mu_0\chi^2H^2$ characterizes the ratio of viscous *vs.* magnetic interactions [11], where $\eta = 10^{-3}\,\mathrm{Nsm}^{-2}$ denotes the water viscosity. The viscous dissipated power $P_{visc} \propto r^3\eta\Omega^2$ cannot exceed the driving magnetic power $P_{magn} \propto ra^2\mu_0\chi^2H^2\Omega$ such that the shear rates must be always smaller than

$$\frac{\Omega}{\omega} < \frac{a^2}{r^2}\mathcal{M}^{-1}. \qquad (2)$$

If $\mathcal{M}$ is low eq. (2) can be satisfied at shear rates $\Omega = \omega$ for conformations with particle separations $r < a\mathcal{M}^{-1/2}$ and the motion is synchronous with the magnetic field. Hence for $\mathcal{M} < 1$ the time-dependent dipolar energy,

$$W = -2\frac{\mu_0}{4\pi}m^2P_2(\cos\varphi(t))/r(t)^3, \qquad (3)$$

can be minimized by an instantaneous minimal conformation $\varphi(t) = \varphi_0$ of the particles that synchronously rotates with the field and the magnetic moment. Here $\varphi(t)$ denotes the angle between the magnetic field and the particle separation and $P_2(\cos\varphi)$ is the second-order Legendre polynomial. Instantaneous minimal conformations are pearl chains oriented parallel to the field.

Increasing $\mathcal{M}$ (*i.e.*, ω) the synchronous rotation is possible only for clusters with smaller size, while larger assemblies fragment into smaller assemblies. The shape of synchronously rotating assemblies and their fragmentation upon adiabatic increase of $\mathcal{M}$ have been studied in detail in the literature [12]. Here we are interested in the dynamics when suddenly switching to very large $\mathcal{M}$, where even the smallest fragments cannot follow the field. If $\mathcal{M}$ is very large, $\mathcal{M} > \mathcal{M}_c \approx 1$, synchronous shear rates can no longer be supported and the time scale of the motion of the particles separates from the time scale of the magnetic field,

$$\frac{\Omega}{\omega} = 1 - \sqrt{1 - \left(\frac{\mathcal{M}_c}{\mathcal{M}}\right)^2}. \qquad (4)$$

At high $\mathcal{M}$ the magnetic dipole interaction between the particles can be averaged over a period of the magnetic field rotation at essentially fixed particle positions,

$$\bar{W} = -\frac{\mu_0}{4\pi}\overline{\mathbf{m}(\mathbf{r}_1(t))\mathbf{m}(\mathbf{r}_2(t))}:\frac{3\mathbf{r}(t)\mathbf{r}(t) - r^2(t)\mathbf{1}}{r^5(t)}, \qquad (5)$$

where the bar denotes the time average over one period. Conformations at high $\mathcal{M}$ hence minimize the time-averaged dipole interaction in eq. (5). For a magnetic field rotating around the z-axis the time-averaged outer vector product of the magnetic moments is $\overline{\mathbf{m}(\mathbf{r}_1(t))\mathbf{m}(\mathbf{r}_2(t))} = m^2(\mathbf{e}_x\mathbf{e}_x + \mathbf{e}_y\mathbf{e}_y)/2$ and the dipole energy between the particles reads

$$\bar{W} = \frac{\mu_0}{4\pi}m^2P_2(\cos\vartheta)/r^3(t), \qquad (6)$$

with ϑ the angle between the particle separation vector and the axis of rotation. Minimal dipole energy conformations therefore correspond to clusters in the plane of rotation $\vartheta = \pi/2$. Note that the structure of eq. (3) and eq. (6) only differ in sign and a factor of 2, as well as in the meaning of the angle in the second-order Legendre polynomial. Thus, a field rotating at high frequency compared to a static magnetic field just reverses the role of attraction and repulsion. The static dipole interaction is attractive along the principal axis (defined by the magnetic field) and repulsive in the plane perpendicular to it. The time-averaged dipolar interaction is repulsive along the principal axis (defined by the rotation axis) and attractive in the plane perpendicular to it.

To assemble particles into a compact cluster, we suddenly switch the magnetic field from a static to a rotating in-plane field,

$$\mathbf{H}(t) = \begin{cases} H\mathbf{e}_x, & \text{for } t < 0, \\ H(\cos\omega t\,\mathbf{e}_x + \sin\omega t\,\mathbf{e}_y), & \text{for } t > 0, \end{cases} \qquad (7)$$

where the electronic switching time ($\sim 20\,\mathrm{ms}$) of our wave generator is much faster than the Brownian self-diffusion time (56 s) footnote[1].

We observe two different transient scenarios for the paramagnetic colloids, depending on the value of $\mathcal{M}$. At low $\mathcal{M}$, when switching to the rotating field, the pearl chains fragment into small rotating assemblies. These small clusters with particle separations $r < a\mathcal{M}^{-1/2}$ synchronously rotate with the external field and attract each other to reassemble into a larger circular cluster. For $\mathcal{M} \gg 1$ no fragmentation of the pearl chains is observed. Instead, the chains start to bend in opposite directions on their two ends until the extremes of the chain form two equilateral triangles with the two adjacent particles (fig. 1, $t = 1\,\mathrm{s}$). These equilateral triangles are the nucleation seeds of two 2D clusters that start to grow at the expense of the pearl chain by rolling up the chain from two sides (fig. 1, $t > 1\,\mathrm{s}$). We describe the chain dynamics in terms of the curve $\mathbf{x}(s,t)$, where s denotes the arc length along the curling chain. The curvature $\kappa(s,t) = |\partial^2\mathbf{x}/\partial s^2|$ measures the shape of the curved chain and the bending rate $\dot{\kappa}(s,t) = \partial\kappa/\partial t$ measures the change in shape upon bending. We use video-microscopy and particle tracking

[1] The paramagnetic colloids have self-diffusion coefficient $D = 0.14\,\mu\mathrm{m}^2\,\mathrm{s}^{-1}$ and the time to diffuse double of their size d is $\tau = d^2/D$.

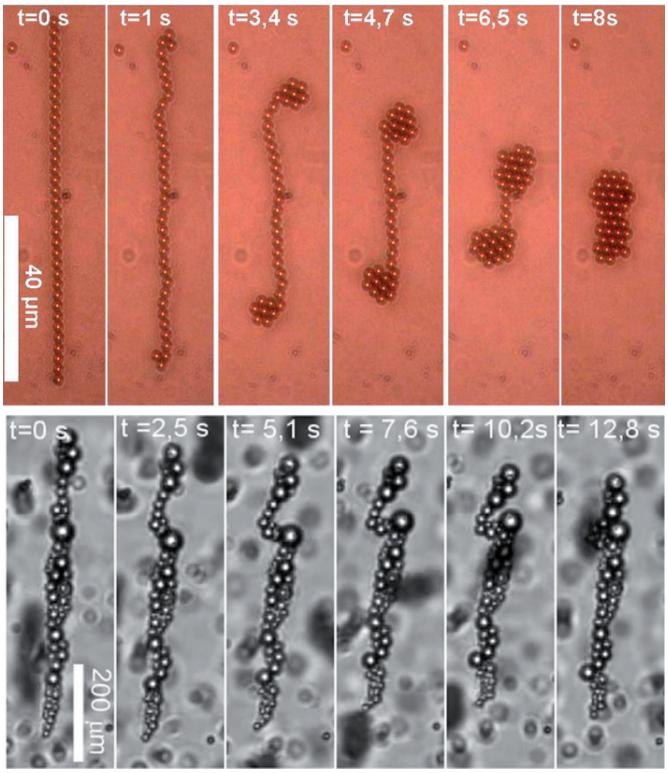

Fig. 1: (Colour on-line) Top: conformation of a pearl chain of 35 paramagnetic particles as a function of time in a rotating magnetic field ($H = 900\,\mathrm{A/m}$, $\omega = 113\,\mathrm{s}^{-1}$). Bottom: conformation of a pearl chain of ferrofluid droplets as a function of time ($H = 1600\,\mathrm{A/m}$, $\omega = 113\,\mathrm{s}^{-1}$). In both experiments the rotating field is switched on at $t = 0\,\mathrm{s}$. See the supplementary movie `ad_1.avi`. The folding is irreversible and a switching back from the rotating to the static magnetic field results in different conformational changes.

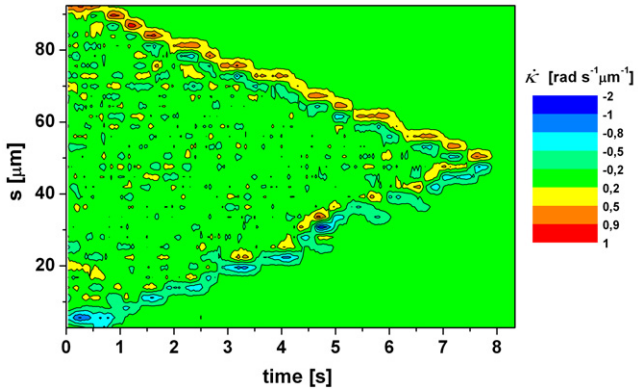

Fig. 2: (Colour on-line) Contour plot of the bending rate $\dot{\kappa}(s,t)$ as a function of the arc-length s along the chain of paramagnetic colloids and the time t.

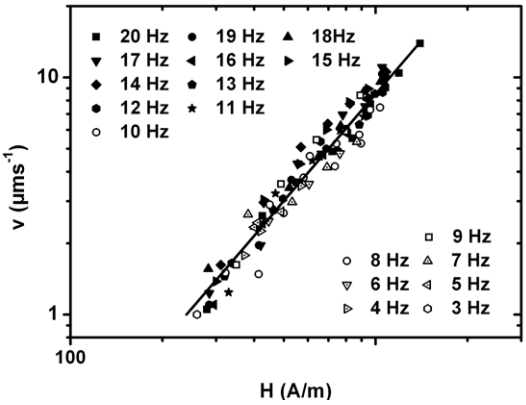

Fig. 3: Bending soliton velocity v as a function of the magnetic field strength H for different frequencies $\nu = \omega/2\pi$ of the field rotation. The solid line is a fit according to eq. (8).

routines to obtain the individual particle position and extract $\dot{\kappa}(s,t)$. The bending rate along the chain as a function of time is shown in fig. 2. Initially the bending rate peaks with opposite signs at the two ends of the chain. Then the two peaks move with constant speed $v = 7.6\,\mu\mathrm{m\,s}^{-1}$ (the step-like features in the peaks are due to the discreteness of the colloids) into the middle of the chain. When the bending soliton passes over a particular position in the chain this position absorbs to the rolling 2D cluster. From the contour plot of the bending rate follows that the pearl chain is subject to weak bending fluctuations which rattle the pearl chain before it absorbs to one of the two rolling clusters where the bending fluctuations cease. Moreover, the 2D cluster shows an increased rigidity with respect to the pearl chain.

In fig. 3 we plot the speed v of the bending soliton *vs.* the field amplitude H for different field frequencies $\nu = \omega/2\pi$. The soliton speed scales like

$$v \propto \omega^0 H^{-3/2}, \tag{8}$$

and is thus independent of ω, showing a scaling exponent with H smaller than the exponent 2 occurring in the dipolar interaction (cf. eq. (3)). We measure the length of the pathway in conformational space as the average of the path lengths of the individual particles, *e.g.*:

$$\mathcal{L} = \frac{1}{L}\int_0^L \mathrm{d}s \int \mathrm{d}t\,|\dot{\mathbf{x}}(s,t)|. \tag{9}$$

The pathway chosen by the particle chain is not the shortest path from a chain toward a cluster. In fig. 4 we plot the dipolar internal energy U of an N-particle system along two different pathways. The first pathway of length $\mathcal{L}_{sol} = 40\,\mu\mathrm{m}$ corresponds to the transition of the particle chain to the cluster via the bending solitons. The second pathway of length $\mathcal{L}_{buck} = 25\,\mu\mathrm{m}$ is a transition of the chain to the cluster via a buckling of the chain. Both pathways end up in equivalent clusters and the dipolar energy monotonously decreases with the path length. Although the buckling takes a shorter path with larger driving force ($F = -\partial U/\partial\mathcal{L} = 17\,\mathrm{fN}$) than for the bending soliton ($F = 10\,\mathrm{fN}$), the particle chain takes the pathway of the bending soliton. The chosen pathway and the behaviour of the bending solitons can be understood when considering the hydrodynamic friction arising along the

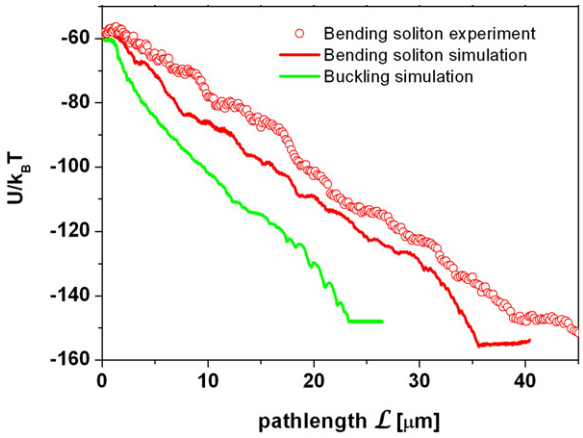

Fig. 4: (Colour on-line) Time-averaged dipolar energy of a 35-particle assembly changing from an extended chain to a cluster along two different pathways. The simulations (straight lines) are computed assuming pairwise additivity of the dipole interaction. The pathway of the steepest descent corresponds to a buckling of the chain. The experimentally observed pathway (circles) of the bending soliton is longer and corresponds to a smaller driving force. The longer pathway is preferred because of the rolling friction between the particles is lower than the sliding friction.

different pathways. Buckling of the chain requires shear flow in the gap region between all consecutive paramagnetic particles. The particles following the bending soliton pathway can avoid relative motion between the surfaces of adjacent particles by rolling on each other. Only at the position of the bending soliton, where the particle chain is wrapped onto the cluster significant shear flow is produced by pumping out the fluid between the chain and the cluster. The gap region between two adjacent particles is dictated by the balance of magnetic dipolar attractions and electrostatic double-layer repulsion, thus it is of the order of the Debye length ($\sim$100 nm) and much smaller than the radius a of the particles. The hydrodynamic friction in such region diverges with vanishing gap width and therefore dominates over the hydrodynamic friction that the particles have with the *free water*. This explains why the speed of the soliton does not change while moving along the particle chain. The driving force is roughly constant and the geometry near the bending soliton does not change. Hence the friction of the squeeze flow near the bending soliton remains similar. The friction with the *free water* that increases with the size of the cluster can be neglected. It would result in a decreasing soliton velocity. Higher magnetic fields increase the attraction between the particles and narrow the gaps between the particles. A smaller gap increases the friction for the relative particle motion and hence the friction coefficient ζ increases with the magnetic field. The speed of the bending soliton $v = F/\zeta$ is the ratio of the driving dipolar force $F \propto H^2$ and the friction coefficient. A friction coefficient scaling like $\zeta \propto H^{1/2}$ is consistent with the experimental scaling in eq. (8) for the bending soliton velocity.

We could not directly visualize the rolling of the beads on top of each other. However, indirect evidence is obtained by comparing the folding of solid colloids to that of liquid droplets. The buckling pathway does not require extensive shear flow if we replace the rigid magnetic particles with ferrofluid droplets. Such droplets can be considered to have a free droplet surface when their size a_{drop} exceeds the viscous length scale $a_{drop} > \eta_s/\eta \approx 1\,\mu$m, where η_s denotes the surface shear viscosity of the droplet [13]. Convection rolls inside the magnetic droplets reduce the friction between the adjacent surfaces of the droplets. Figure 1 (bottom) shows the transition from a polydisperse pearl chain of ferrofluid droplets towards a cluster. Contrary to the rigid particles the ferrofluid droplets follow the shorter buckling pathway. We have performed also experiments with bidisperse particles to check whether polydispersity could affect the chosen pathway since the ferrofluid droplets are polydisperse, but we observe no difference with the monodisperse case.

We support the experimental results with fluid particle simulations [14,15] where the particles are treated as a parts of the liquid of much larger viscosity. We also simulated the dynamics of "slippery" beads by using the method of hydrodynamic interactions between point-like particle in the Rotne-Prager approximation [16]. These simulations confirm the importance of friction for the choice of the folding pathway. The experimental and simulation videos `ad_1.avi` show the dynamics of the particles in both systems.

In conclusion we have shown that in our colloidal system the kinetics of folding is dominated by the different friction arising along the slopes of the energy landscape rather than by transition rates over flat saddle points. The short pathway from a pearl chain toward a cluster via the buckling of the chain is suppressed by the friction of relative motion between the adjacent surfaces of the particles and not by presence of barriers in the energy landscape. The system therefore avoids the pathway of the steepest descent and chooses an alternative longer pathway via the bending soliton that minimizes the friction.

* * *

This work was supported by the German Science Foundation via the priority program 1164 and the center of excellence 840 and through the program "Juan de la Cierva" (JCI-200904192). We thank J. Bammert and P. Peyla for helpful discussion.

REFERENCES

[1] Anfinsen C. B. and Scheraga H. A., *Adv. Protein Chem.*, **29** (1975) 205; Onuchic J. N., Luthey-Schulten Z. and Wolynes P. G., *Annu. Rev. Phys. Chem.*, **48** (1997) 545; Nolting B., *Protein Folding Kinetics: Biophysical Methods* (Springer, Berlin) 1999;

Eaton W. A. *et al.*, *Annu. Rev. Biophys. Biomol. Struct.*, **29** (2000) 327; Daggett V. and Fersht A., *Nat. Rev. Mol. Cell Biol.*, **4** (2003) 497.
[2] Bryngelson J. D. *et al.*, *Proteins: Struct. Funct. Genetics*, **21** (1995) 167.
[3] Kikuchi N. *et al.*, *Phys. Rev. E*, **71** (2005) 061804.
[4] Cieplak M. and Niewieczerzał S., *J. Chem Phys.*, **130** (2009) 124906.
[5] van Blaaderen A., Ruel R. and Wiltzius P., *Nature*, **385** (1997) 321.
[6] Weeks E. R. *et al.*, *Science*, **287** (2000) 627.
[7] Osterman N. *et al.*, *Phys. Rev. Lett.*, **103** (2009) 228301.
[8] Baumgartl J., Zvyagolskaya M. and Bechinger C., *Phys. Rev. Lett.*, **99** (2007) 205503.
[9] Toussaint R., Helgesen G. and Flekkøy E. G., *Phys. Rev. Lett.*, **93** (2004) 108304.
[10] Tierno P., Muruganathan R. and Fischer T. M., *Phys. Rev. Lett.*, **98** (2007) 028301; Tierno P. *et al.*, *Phys. Rev. E*, **79** (2009) 021501.
[11] Gast A. P. and Zukoski C. F., *Adv. Colloid Interface Sci.*, **30** (1989) 153.
[12] Melle S. *et al.*, *Phys. Rev. E*, **68** (2003) 041503; Biswal S. L. and Gast A. P., *Phys. Rev. E*, **69** (2004) 041406; Černák J. and Helgesen G., *Phys. Rev. E*, **78** (2008) 061401.
[13] Levich V. G., *Physicochemical Hydrodynamics* (Prentice-Hall, Englewood Cliffs, NJ) 1962.
[14] Tanaka H. and Araki T., *Phys. Rev. Lett.*, **85** (2000) 1338.
[15] Peyla P., *EPL*, **80** (2007) 34001.
[16] Rotne J. and Prager S., *J. Chem. Phys.*, **50** (1969) 4831.